



The impact of degassing on the oxidation state of basaltic magmas: A case study of Kīlauea volcano



Yves Moussallam^{a,*}, Marie Edmonds^b, Bruno Scaillet^c, Nial Peters^d, Emanuela Gennaro^c, Issy Sides^b, Clive Oppenheimer^d

^a Geosciences Research Division, Scripps Institution of Oceanography, UCSD, La Jolla, CA 92093-0244, USA

^b Department of Earth Sciences, University of Cambridge, Downing Street, Cambridge, CB2 3EQ, UK

^c ISTO, UMR 7327, Université d'Orléans-CNRS-BRGM, 1A rue de la Férollerie, 45071 Orléans cedex 2, France

^d Department of Geography, University of Cambridge, Downing Place, Cambridge, CB2 3EN, UK

ARTICLE INFO

Article history:

Received 29 March 2016

Received in revised form 17 May 2016

Accepted 17 June 2016

Available online 12 July 2016

Editor: T.A. Mather

Keywords:

oxygen fugacity

sulfur

degassing

XANES

melt inclusions

CO₂

ABSTRACT

Volcanic emissions link the oxidation state of the Earth's mantle to the composition of the atmosphere. Whether the oxidation state of an ascending magma follows a redox buffer – hence preserving mantle conditions – or deviates as a consequence of degassing remains under debate. Thus, further progress is required before erupted basalts can be used to infer the redox state of the upper mantle or the composition of their co-emitted gases to the atmosphere. Here we present the results of X-ray absorption near-edge structure (XANES) spectroscopy at the iron K-edge carried out for a series of melt inclusions and matrix glasses from ejecta associated with three eruptions of Kīlauea volcano (Hawai'i). We show that the oxidation state of these melts is strongly correlated with their volatile content, particularly in respect of water and sulfur contents. We argue that sulfur degassing has played a major role in the observed reduction of iron in the melt, while the degassing of H₂O and CO₂ appears to have had a negligible effect on the melt oxidation state under the conditions investigated. Using gas–melt equilibrium degassing models, we relate the oxidation state of the melt to the composition of the gases emitted at Kīlauea. Our measurements and modelling yield a lower constraint on the oxygen fugacity of the mantle source beneath Kīlauea volcano, which we infer to be near the nickel nickel-oxide (NNO) buffer. Our findings should be widely applicable to other basaltic systems and we predict that the oxidation state of the mantle underneath most hotspot volcanoes is more oxidised than that of the associated lavas. We also suggest that whether the oxidation states of a basalt (in particular MORB) reflects that of its source, is primarily determined by the extent of sulfur degassing.

© 2016 The Author(s). Published by Elsevier B.V. This is an open access article under the CC BY license (<http://creativecommons.org/licenses/by/4.0/>).

1. Introduction

The redox state of basalts, and especially of mid ocean ridge basalts (MORBs) has been proposed to be a direct reflection of the oxidation state of their source region (e.g. Carmichael and Ghiorso, 1986; Carmichael, 1991; Bezos and Humler, 2005; Lee et al., 2005; Cottrell and Kelley, 2011). Very slight variations in the oxidation state of MORBs and, by inference, the oxidation state of the upper mantle, have been used to support far-reaching implications of element cycling at the planetary scale (Cottrell and Kelley, 2013; Shorttle et al., 2015). There are several reasons, however, why the oxidation state of erupted MORBs might not reflect mantle conditions. Nearly all MORBs are vapour-saturated and are therefore

significantly degassed by the time they erupt (e.g. Moore, 1979; Dixon et al., 1988; Bottinga and Javoy, 1990).

The degassing of volatile species has long been suggested to affect melt oxidation state. The degassing of H₂O and H₂ is predicted to result in a net oxidation of the melt (Sato and Wright, 1966; Sato, 1978; Mathez, 1984; Holloway, 2004); evidence of this process has been observed in rhyolitic melt decompression experiments (Humphreys et al., 2015) but its occurrence in nature remains questionable (Waters and Lange, 2016). The degassing of carbon monoxide may oxidise the melt (Mathez, 1984), while the degassing of sulfur species can oxidise or reduce melts depending on sulfur speciation in the melt (S^{2−} or S⁶⁺) and fluid phase (H₂S, or SO₂) (Anderson and Wright, 1972; Carmichael, 1991; Gerlach, 1993; Gaillard and Scaillet, 2009; Métrich et al., 2009; Gaillard et al., 2011, 2015; Kelley and Cottrell, 2012; Moussallam et al., 2014).

* Corresponding author.

E-mail address: ymoussallam@ucsd.edu (Y. Moussallam).

Similar to MORB, the oxidation state of the mantle feeding ocean island basaltic (OIB) volcanoes has been inferred from the oxidation state of erupted lavas and gases. In Hawai'i these approaches have led to disagreement, with the initial oxidation state of parental Hawaiian magmas argued to be close to the magnetite–wüstite (MW) buffer (Roeder et al., 2003; Rhodes and Vollinger, 2005); close to the nickel nickel-oxide (NNO) buffer (Helz and Thornber, 1987); or close to the quartz–fayalite–magnetite (QFM) buffer (Fudali, 1965; Peck and Wright, 1966; Sato and Wright, 1966; Wright and Weiblen, 1968; Anderson and Wright, 1972; Gerlach, 1980, 1993; Carmichael and Ghiorso, 1986). To date the oxidation state of the Hawaiian mantle plume remains undetermined.

Here, we examine a series of olivine-hosted melt inclusions (MI) and matrix glasses from tephra erupted during three eruptions of Kīlauea volcano. These MI and glasses provide samples of the melt tapped at different degassing stages and have already been extensively characterised in terms of major, trace and volatile element compositions (Edmonds et al., 2013; Sides et al., 2014). We present X-ray absorption near-edge structure (XANES) spectroscopy measurements at the iron K-edge on a subset of these glasses to investigate the link between melt oxidation state and degassing, thereby enabling us to extrapolate back to the mantle oxidation state of pristine, undegassed Kīlauea basalt.

2. Methodology

We began our investigation with a sample set of 387 MI and 175 glasses from 25 historical eruptions at Kīlauea, which had previously been analysed for major, trace and volatile elements by EMP, SIMS and LA-ICPMS by Sides et al. (2014) and Edmonds et al. (2013). From this sample set we selected 20 MI and 24 matrix glasses for XANES spectroscopy measurements at the iron K-edge. The MI were selected based on their calculated amount of post-entrapment crystallisation (PEC) (i.e. from the 387 MI of the sample set we selected the ones with the lowest amount of PEC). This narrowed the sample set to three eruptions, which took place in 2010, 2008 and 1885.

The matrix glasses were then taken from corresponding eruptions. The 2010 and 2008 samples are from transient explosive (gas-rich, melt-poor) eruptions and consist of pumiceous bombs/lapilli and lithics, while the 1885 samples relate to an effusive eruption and taken from the upper 1–1.5 cm of the glass-rich vesicular rope texture on pāhoehoe lava flow surfaces. The melt composition of these three eruptions is representative of typical Kīlauea basalt (Fig. S1). The selected samples were re-polished to remove the spot left by previous SIMS analysis and polished on the reverse side in order to obtain doubly-exposed wafers with at least a $10 \times 10 \mu\text{m}^2$ obstruction-free area through the inclusion. Fig. 1 shows the typical morphology of an olivine-hosted MI and its surrounding glass. The analysed inclusions vary in size from 20 to 60 μm across and consist of brown-coloured transparent glass of ovoid shape located throughout the crystal.

2.1. XANES data acquisition

All samples were analysed on Beamline I18 at the diamond light source (DLS) using Fe K-edge XANES (X-ray absorption near-edge structure spectroscopy). The X-rays were focused with Kirkpatrick–Baez mirrors down to $2 \mu\text{m}$ (horizontal) $\times 2.5 \mu\text{m}$ (vertical) beam size. The beamline utilises a liquid nitrogen-cooled double-crystal monochromator with silicon crystals and Si(333) reflection was used to increase the energy resolution. Measurements were performed in fluorescence mode and the energy-dispersive detector used was a 6-element SGX SORTECH silicon drift detector positioned at 90° to the incident X-ray beam. The sample was

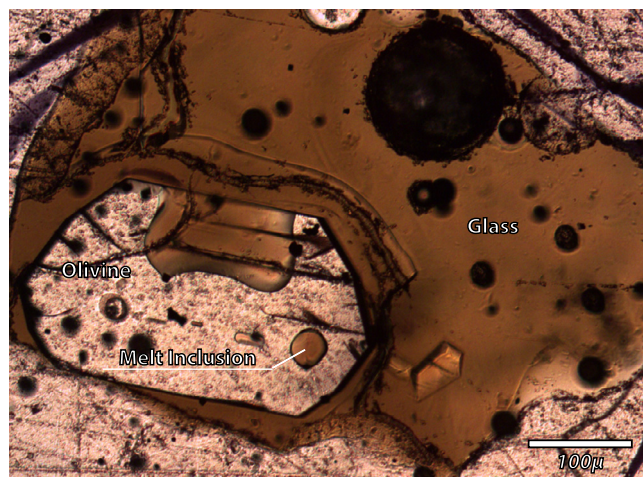


Fig. 1. Transmitted light photomicrograph of an olivine hosted melt inclusion from the 2010 eruption (sample S3-56). Rapid quenching of the MI and matrix glass is evident from the absence of microlites and is representative of all three eruptions investigated.

positioned so that the normal to the sample surface was at 10° to the incident X-ray beam to improve the horizontal resolution and reduce potential self-absorption effects. The incident X-ray beam was filtered with Al foils (varying in thickness from 0.025 to 0.1 mm) to keep the detector count rate within the linear response region and to remove the effect of beam damage on the sample. The energy step sizes and dwell times used are given in Table S1.

2.2. Beam damage

Focused beams of X-rays have been shown to either reduce (Wilke et al., 2008; Métrich et al., 2009) or oxidise (Moussallam et al., 2014) sulfur during XANES analyses on a timescale of minutes. The effect of beam damage at the Fe K-edge has been investigated in several studies (Cottrell et al., 2009; Moussallam et al., 2014; Shorttle et al., 2015). Cottrell et al. (2009) and Moussallam et al. (2014) found no effect of prolonged beam-time on the Fe speciation under their set of analytical conditions. Shorttle et al. (2015) found that under certain analytical conditions (without attenuation of the beam) a small amount of photo-oxidation could be generated over the first 12 min of sample exposure to the beam. In order to determine if beam damage was occurring under our analytical conditions we acquired five successive spectra on a natural Kīlauea glass sample. Spectra were obtained using a “fast-scanning” mode such that each spectrum took about 4.5 min to acquire. Although “fast-scanning” results in lower resolution spectra it allows investigation of time-dependent beam damage. Apart from shorter dwell time, these spectra were acquired under the same analytical conditions as the rest of the sample set and using an Al plate of 0.025 mm. Fig. S2 shows that all five spectra are nearly identical and hence that no significant beam damage is to be expected in our analyses.

2.3. Spectral processing and $\text{Fe}^{3+}/\Sigma\text{Fe}$ calibration

The pre-edge region (7110–7118 eV) on a XANES spectrum at the Fe K-edge corresponds to the $1s \rightarrow 3d$ electronic transition. The pre-edge region was fitted using a combination of a linear function and a damped harmonic oscillator function (DHO) to fit the baseline (Cottrell et al., 2009; Moussallam et al., 2014) (Fig. S3). The centroid (area-weighted average) of the background-subtracted pre-edge region was then calculated and parametrised against the Fe valence state. We used the NMNH 117393 basalt reference glasses (Cottrell et al., 2009) loaned by the Smithsonian Institution

Download English Version:

<https://daneshyari.com/en/article/6427311>

Download Persian Version:

<https://daneshyari.com/article/6427311>

[Daneshyari.com](https://daneshyari.com)